

Nanoscale ferromagnet-superconductor-ferromagnet switches controlled by magnetization orientation

Klaus Halterman^{1,*} and Oriol T. Valls^{2,†}

¹*Physics and Computational Sciences, Research and Engineering Sciences Department,
Naval Air Warfare Center, China Lake, California 93555*

²*School of Physics and Astronomy and Minnesota Supercomputer Institute,
University of Minnesota, Minneapolis, Minnesota 55455*

(Dated: January 30, 2022)

We study clean ferromagnet-superconductor-ferromagnet (FSF) nanostructures in which the magnetization of the F layers can be parallel (P) or antiparallel (AP). We consider the case where the thickness of the S layer is of order of the coherence length, with thinner F layers. We find that reversing the direction of the magnetization in one of the F layers leads in general to drastic changes in the superconductor's state. Under a wide variety of conditions, the AP geometry favors superconductivity. Magnetization reversal in one of the F layers can lead to the superconductivity turning on and off, or to switching between different states. Our results are obtained via self consistent solution of the Bogoliubov-de Gennes equations and evaluation of the condensation energies of the system.

PACS numbers: 74.45.+c, 74.25.Fy, 74.78.Fk

Introduction: Within the emerging field of spintronics¹ considerable interest has developed in devices in which proximity effects are used to control the superconductivity via the spin degree of freedom in ferromagnet (F) and superconductor (S) layered systems. A large part of the motivation for this interest follows from earlier studies of systems that involve non-magnetic normal metal layers sandwiched between two ferromagnetic layers² (FNF geometry). In such devices the resistance of the system can change substantially in the presence of a perturbing magnetic field. This change mainly arises from the spin-dependent scattering at the interfaces. The ensuing giant magnetoresistance (GMR) effect is found in spin-valves and magnetic multilayers where the relative orientations of the magnetization in alternate ferromagnetic layers change as a function of an applied field. If the local magnetization orientations are antiparallel (AP) the scattering will be stronger for a particular spin component, but if the magnetization vectors are aligned the more weakly scattered spin component carries the current with a lower resistivity.

If the nonmagnetic insert is replaced by a thin superconductor, resulting in a ferromagnet-superconductor-ferromagnet (FSF) junction, a different type of spin-valve or spin-switch can be created³. The proximity effects arising from the mutual influence of the magnetic and superconducting order parameters embody a variety of novel spin-valve effects and device concepts, including high density nonvolatile memory,⁴ and magnetic sensors. The mechanism behind such devices is ultimately based⁵ on the damped oscillatory nature of the superconductor order parameter in the F regions, and the associated magnetic correlations and destruction of superconductivity in the S layer. In the transport regime, and with AP alignment of the magnetizations in the F layers, a nonequilibrium spin density can accumulate in the superconductor^{6,7,8}, destroying the gap and result-

ing in a higher resistance state for a given temperature.⁹ Thus the superconducting correlations are controlled by the relative magnetization orientation in the F layers. Also, quasiclassical thermodynamic considerations indicate that the transition temperature, T_c , can be modified in a controlled way, thus allowing supercurrent to flow in a predictable manner,^{5,10,11,12} yielding another type of spin switch. The superconducting order parameter and T_c in this case are again greatest when the the magnets are in the AP configuration, a result shown to hold for atomic thickness FSF layers as well.¹³ When the superconducting system goes normal, the phase transition is second order for AP magnetizations in the F layers and can be first order for parallel (P) magnetizations if the F layers are thin enough and the interface transparency is high.¹⁴ If the outer ferromagnets are semiconducting insulators, the T_c variations have different signatures depending on whether the superconductor is in the singlet or triplet state.¹⁰ An absolute spin-valve effect can occur at spin-active interfaces in which the tunneling current is finite for a range of voltages.¹⁵

These types of devices are in general most effective, and the effects most pronounced, for junctions with clean interfaces and thin superconductors.¹¹ The lithographic, sputtering, and epitaxial methods used in spin-switch fabrication permit the creation of structures as thin as a few atomic layers that have atomically flat interfaces. Moreover, high quality magnetic and nonmagnetic metallic films with an electron mean free path exceeding 150 Å can also be readily fabricated. One of the earliest experiments using FSF junctions involved CuNi/Nb/CuNi films, and a magnetization direction dependence on T_c was reported.³ A spin switch was recently investigated using La_{0.7}Ca_{0.3}MnO₃/YBa₂Cu₃O₇ superlattices that had large magnetoresistance when in the superconducting state.⁹ Spin valve core structures involving Nb/CuNi sandwiches have also very recently¹⁶

been reported. It is possible, in an FSF sandwich with AP magnetizations, for the electron in one of the magnets to be Andreev reflected as a hole of the opposite spin in the other ferromagnet.¹⁷ This process of crossed Andreev reflection is believed to be behind the results of experiments involving subgap transport in Al/Fe hybrids.¹⁸ An enhancement of the critical current and T_c in Nb/Co was observed and was attributed to a reduced exchange interaction in the domain structure of Co.¹⁹ Likewise, a type of spin-switch involving Nb/Permalloy layers revealed through transport measurements, a decrease in the suppression of superconductivity.²⁰ It was argued that the superconductivity is increased when the magnetic domains are oriented differently, effectively averaging in a way that reduces the effects of the exchange field.

Spurred by these important advances, we investigate here the effect of reversing one of the magnetizations in clean FSF nanojunctions. We consider the relevant case where the coupling between the S and F regions is appreciable, namely a thin S layer (of order of the BCS coherence length ξ_0) and relatively large magnetic exchange fields. Our results are based upon numerical self-consistent²¹ solution of the microscopic Bogoliubov-de Gennes (BdG) equations. This method is most appropriate for the situation described above. We calculate the pair potential $\Delta(\mathbf{r})$, the condensation energy, and the local density of states (LDOS) for both the P and AP magnetization configurations, over a range of values of the relevant parameters. Our analysis will demonstrate that under many conditions the system can be made to switch from a superconducting state to a normal one, at low temperatures, by flipping the (collinear) magnetization orientation in one of the F layers, which can be achieved via an applied field. This will be illustrated by calculating the condensation energy as a function of ferromagnet thickness and exchange energy. We find that the AP state is always the lowest energy state, and thus the most favorable. We conclude that the proximity effects that occur with P magnetization in successive F layers become substantially modified when adjacent F layers have AP magnetization alignment. The pair amplitude and LDOS also display experimentally discernible characteristics that depend on whether the magnets are in the P or AP configuration.

Methods: The equations relevant to the microscopic theory of inhomogeneous superconductivity are the Bogoliubov-de Gennes (BdG) equations.²² We consider here an FSF structure translationally invariant in the $x - y$ plane, with interfaces normal to the z direction. We assume parabolic bands with bandwidths E_F in the S layer and $E_{F\pm} \equiv E_F \pm h_0$ in the magnet, where h_0 is the Stoner exchange field. In the P geometry the sign of h_0 is the same in both layers, while in the AP geometry it is²³ the opposite. The dimensionless parameter $I \equiv h_0/E_F$ characterizes the magnetic strength. We include interface scattering characterized by delta functions of strength H (dimensionless strength $H_B \equiv mH/k_F$). We have writ-

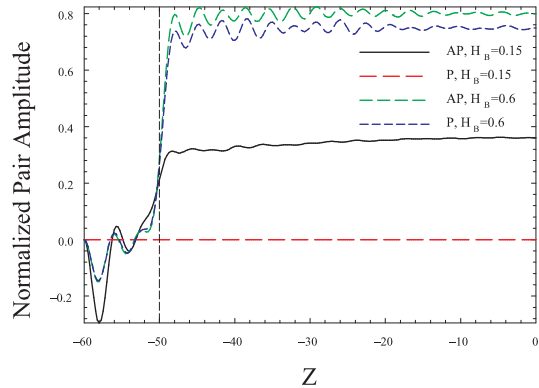


FIG. 1: (Color online) The spatially dependent pair amplitude (normalized to its $T = 0$ bulk value) for a FSF trilayer, plotted vs. $Z \equiv k_F z$. The contrasting cases where the magnetizations in the F layers are parallel (label P), or antiparallel (label AP) are shown. Because of symmetry, only half of the sample is included. Each magnet has width $D_F \equiv k_F d_F = 10$. The dashed vertical line is at the F/S interface. Two values of the scattering strength H_B are considered. For the smaller value the pair amplitude vanishes in the P configuration. The pair amplitude is always larger in the AP configuration. The exchange parameter is $I = 0.2$.

ten the BdG equations in this geometry and with these assumptions in previous^{21,24} work, where we have also discussed²⁵ the specific numerical methodology we use. It is therefore unnecessary to repeat these derivations here. The exact quasiparticle energies and amplitudes are thus obtained by repeated iteration of the BdG equations and the associated self-consistency condition for $\Delta(z)$.

Once the energy spectra and pair potential are found, the condensation free energy, \mathcal{F} , (or, in the $T \rightarrow 0$ limit the condensation energy) can be calculated. This is in principle straightforward, although numerically quite difficult. We use²⁵ a particularly convenient approach^{26,27} which yields for the condensation energy ΔE_0 the result:

$$\Delta E_0 = \sum_{n'} \epsilon_{n'}^0 - \sum_n \epsilon_n + \int_0^d dz \frac{|\Delta(z)|^2}{g}, \quad (1)$$

where g is the BCS coupling constant in S, d the total sample width, ϵ_n and $\epsilon_{n'}^0$ are the free-particle energy spectra corresponding respectively to the superconducting and normal ($\Delta(z) \equiv 0$) states, and the indices denote the appropriate²⁵ quantum numbers. The sums are performed over energies less than the usual cutoff ω_D . Similarly, from the calculated self-consistent eigenvalues and eigenfunctions one can calculate the LDOS, $N(z, \epsilon)$. This quantity is discussed below.

Results: In the geometry we consider, the inner superconductor layer of width d_S is sandwiched between two ferromagnet layers of equal width, d_F . The thickness d_S is chosen to be $d_S = \xi_0$, and we take $k_F \xi_0 = 100$ and $\omega_D = 0.04 E_F$. All results correspond to low temper-

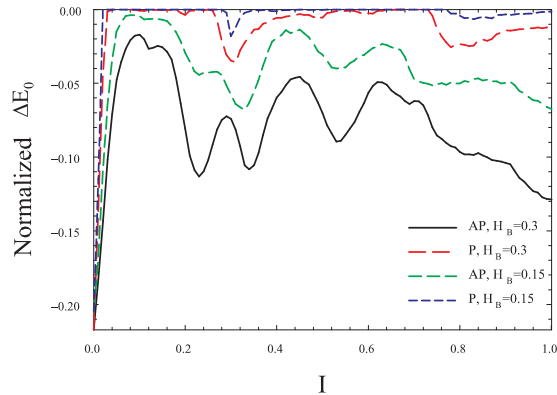


FIG. 2: (Color online) The condensation energy, ΔE_0 , normalized to $N(0)\Delta_0^2$, plotted vs I for two values of H_B . The oscillatory behavior is complicated, but for both H_B values the AP state is favored over the whole I range.

ature, $T = 0.01T_c$.

In Fig. 1 we plot the pair amplitude (the average $\langle\hat{\psi}_\downarrow(\mathbf{r})\hat{\psi}_\uparrow(\mathbf{r})\rangle$, where the $\hat{\psi}_\sigma$ are the usual annihilation operators), normalized to its zero temperature bulk value, as a function of dimensionless distance. Results are plotted both for both the P and AP cases. Two values of the interface scattering parameter are considered, a small one ($H_B = 0.15$) when the proximity effect is strong, and a larger one ($H_B = 0.6$) when it is weaker. It is clear that the results depend crucially on the relative magnetization orientation, with the superconducting amplitude being weakest in the P case. The effect is magnified for the smaller H_B value, where interface scattering is reduced. In that case one can see in the figure that the pair amplitude vanishes in the P case, while being quite robust in the AP situation. The superconductivity can thus be *switched on and off* by reversing the magnetization in one of the F layers.

This favoring of the AP configuration is, qualitatively, a very general phenomenon. To see this, it is very convenient to analyze the pair condensation energy (Eq. (1)). The trends in the pair amplitude, such as those in Fig. 1, should be reflected in the condensation energy, which should then be lower (higher in absolute value) in the AP case than in the P configuration. ΔE_0 is shown in the next two figures, normalized to $N(0)\Delta_0^2$ which is twice its bulk zero temperature value. In Fig. 2 this normalized quantity is plotted as a function of I for two values of H_B . The F width is kept fixed at $D_F \equiv k_F d_F = 10$ (recall that $D_S \equiv k_F \xi_0$ always). The entire range of I from the nonmagnetic ($I = 0$) limit to the half metallic case ($I = 1$) is spanned. For all nonzero I , the AP case is always favored. This trend persists even for larger H_B (not shown) where the proximity effect is weaker. At $I = 1$ only one spin band is populated at the Fermi level and consequently $|\Delta E_0|$ is large, as Andreev reflection is depressed and the Cooper pairs are more restricted to the

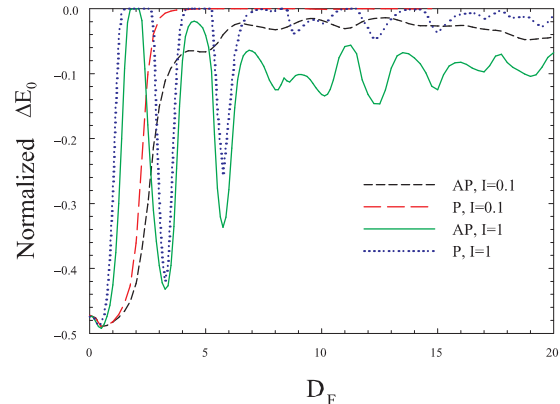


FIG. 3: (Color online) The normalized condensation energy vs. the dimensionless ferromagnet width D_F . Two values of I are considered, as indicated, at $H_B = 0.3$. For a given I , the AP state has lower ΔE_0 over the whole D_F range included.

S region. We also see in the figure that the *difference* in condensation energies for P and AP geometries at fixed thickness is a weak function of I , except at small I .

The AP configuration continues to be preferred when the thickness D_F is varied at constant I . This is shown in Fig. 3, where we plot the normalized ΔE_0 versus D_F . Results for two values of I are plotted, and both P and AP configurations are studied. As $D_F \rightarrow 0$, one is left only with the superconductor and ΔE_0 approaches its bulk value. Increasing D_F causes initially a sharp rise in ΔE_0 . The condensation energy then saturates, exhibiting damped irregular oscillations, reflecting the competition between magnetism and superconductivity. Again, in all cases superconductivity favors the AP configuration. At small I ($I = 0.1$), ΔE_0 for the P configuration vanishes beyond $D_F \gtrsim 4$, while in the half-metallic limit, ΔE_0 is an oscillatory function of D_F . The difference in condensation energies between P and AP configurations at the same I is a weak function of D_F .

The irregular oscillatory behavior in Figs. 2-3 reflects the existence of the characteristic length $\ell = (k_\uparrow - k_\downarrow)^{-1}$ arising from the difference between Fermi wavevectors for up and down spins in the F layers. Such oscillatory behavior depends on the relation between d_F and ℓ . The latter in turn depends on I . Since the ratio ℓ/d_F depends on D_F in a simpler way than on I , the oscillations are best studied in Fig. 3. There one can see that at larger $I = 1$ (hence smaller ℓ), the characteristic oscillations have a shorter spatial period than those at $I = 0.1$. For SFS sandwiches with small D_F one finds²⁴ oscillations in the pair amplitude in F. These can be seen in the left edge of Fig. 1. The situation for ΔE_0 is much more complicated, since oscillations in the pair amplitude are only indirectly reflected there.

The strong modifications to the superconducting state of the sample should be easily detected in measurements of the critical current. These switching effects are also

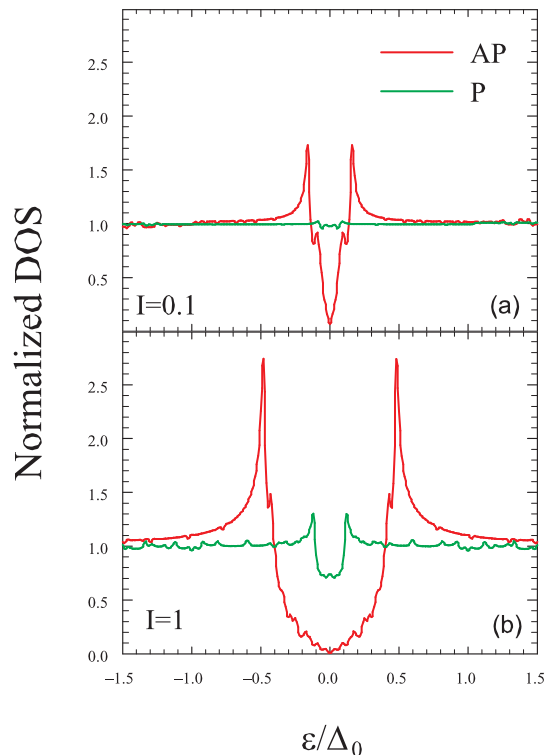


FIG. 4: (Color online) The normalized LDOS (at $D_F = 10$ and $H_B = 0.15$) spatially averaged over the S region and normalized as explained in the text. Results for both P and AP configurations are shown for two I values.

very well reflected in LDOS results. Thus, we show in Fig. 4 the LDOS $N(z, \varepsilon)$ averaged over the S region. The results are normalized to the normal state bulk value.

We display results for two values of I , $D_F = 10$, and $H_B = 0.15$. One can plainly see the difference between P and AP configurations: in the AP case the BCS like peaks are much more prominent and the gap fairly well defined. In the P case no gap exists, although a weak BCS like feature is still visible for $I = 1.0$, while the features flatten out nearly completely at small I ($I = 0.1$), when the system is no longer superconducting, as seen by the vanishing of the condensation energy in this case, (Fig. 2).

The enhancement of superconductivity in the AP configuration is not, as one might naively think, simply a consequence of the magnetic polarizations canceling in the superconductor. As has been found,²¹ the magnetic moment induced in the superconductor by the ferromagnetic contacts penetrates into the S material only a few Fermi wavelengths. We have verified that this is also the case here. Thus, the reasons are more subtle. The weakening of superconductivity by ferromagnetic contacts depends in a complicated way on the amplitudes for electron scattering (both normal and Andreev) at the interfaces. These are to a greater or lesser strength pair breaking. The penetration depth for Cooper pairs into the F material is much smaller than for a normal metal and this is reflected in the interface scattering amplitudes. Our self consistent calculation shows then, that the superconducting state (with $d_S = \xi_0$) can better survive proximity to two F contacts that have opposite polarizations.

Acknowledgments: We thank Paul Barsic for several conversations. This work was supported in part by a grant of HPC resources from ARSC at the University of Alaska Fairbanks as part of the DoD High Performance Computing Modernization Program.

* Electronic address: klaus.halterman@navy.mil

† Electronic address: otvalls@umn.edu

¹ I. Zutic, J. Fabian, and S. Das Sarma, Rev. Mod. Phys. **76**, 323 (2004).

² See section II of Ref. 1 for a review.

³ J. Y. Gu *et al.*, Phys. Rev. Lett. **89**, 267001 (2002).

⁴ S. Oh, D. Youm, and M. R. Beasley, Appl. Phys. Lett. **71**, 2376 (1997).

⁵ L. R. Tagirov, Phys. Rev. Lett. **83**, 2058 (1999).

⁶ S. Takahashi, H. Imamura, and S. Maekawa, Phys. Rev. Lett. **82**, 3911 (1999).

⁷ Z. Zheng *et al.*, Phys. Rev. B **62**, 14326 (2000).

⁸ T. Yamashita *et al.*, Phys. Rev. B **67**, 094515 (2003).

⁹ V. Peña *et al.*, Phys. Rev. Lett. **94**, 057002 (2005).

¹⁰ M. L. Kulić and M. Endres, Phys. Rev. B **62**, 11846 (2000).

¹¹ I. Baladié and A. Buzdin, Phys. Rev. B **67**, 014523 (2003).

¹² C-Y You *et al.*, Phys. Rev. B **70**, 014505 (2004).

¹³ S. Tollis, Phys. Rev. B **69**, 104532 (2004).

¹⁴ S. Tollis, M. Daumens, and A. Buzdin, Phys. Rev. B **71**, 024510 (2005).

¹⁵ D. Huertas-Hernando, Y. V. Nazarov, and W. Belzig, Phys. Rev. Lett. **88**, 047003 (2002).

¹⁶ A. Potenza and C.H. Marrow, cond-mat/0505124 (unpublished) (2005).

¹⁷ R. Mélin, cond-mat/0502021 (unpublished) (2005).

¹⁸ D. Beckmann, H. B. Weber, and H. v. Löhneysen, Phys. Rev. Lett. **93**, 197003 (2004).

¹⁹ R. J. Kinsey, G. Burnell, and M. G. Blamire, IEEE Trans. Appl. Supercond. **11**, 904 (2001).

²⁰ A. Y. Rusanov *et al.*, Phys. Rev. Lett. **93**, 057002 (2004).

²¹ K. Halterman and O.T. Valls, Phys. Rev. B **69**, 014517 (2004).

²² P.G. de Gennes, *Superconductivity of Metals and Alloys* (Addison-Wesley, Reading, MA, 1989).

²³ We consider only the collinear case for h_0 , and no spin-orbit coupling, so that only singlet pairing needs to be included.

²⁴ K. Halterman and O.T. Valls, Phys. Rev. B **65**, 014509 (2002).

²⁵ K. Halterman and O.T. Valls, Phys. Rev. B **70**, 104516 (2004), *ibid.* **66**, 224516 (2002).

²⁶ C.W.J. Beenakker and H. van Houten, *Nanostructures and Mesoscopic Systems*, (Academic, New York, 1992): pp. 481-497.

²⁷ I. Kosztin *et al*, Phys. Rev. B **58**, 9365 (1998).